

The Design and Simulation of Optical Receivers with Capability of AGC, Based on ZnO Crystal Structures using TMM Method

Reza Khodadadi, Samaneh Khodadadi

Abstract – To recognize a ray in the wavelength range of 625 nm to 645 nm with the possibility of AGC (Automatic Gain Control), the conditions have been predicted in a way that using a structure of 21 pairs of crystal layers containing the mixture of oxide and glass with the failure coefficients $n_{ZnO} = 2.0041$, $n_{Glass} = 1.45$ with a pair of air gap layers, the simulation can be carried out. In this optical receiver sensor, the length of channels is 100 nm and the analysis is based on TMM. At particular angles which the gain is more than 70% and the bandwidth is about 1 nm, the incident ray is acceptable and the system output is active; otherwise, the controller will change the direction of the incident angle to the closest one.

Keywords – TMM Analysis, Photonic Crystals, AGC, Optical Receiver, ZnO Thin Films.

I. INTRODUCTION

Considering the fact that using the optical receivers is dependent on their fast time response, so in PIN photodiodes a high power and bandwidth efficiency are defined as their advantages which, in practice, pure width in Si PIN photodiodes is about 40 μm and in InGaAs photodiodes is about 4 μm and also APDs, using a high reverse voltage in the wavelength range of 1.3 μm to 1.55 μm , are highly efficient, reliable, and satisfactory. Because the presented design has been simulated in the wavelength range of 625 nm to 645 nm and has been proportional to the optical sensor SLD1132VS, so in this article, using TMM, a ZnO crystal structure consisting of an array of 21 parallel layers having identical distances from each other ($dL = 100$ nm) and refractive indices of 1.45, 2.0041 is proposed in a way that it is possible to gain through applying a ray as an optical AGC at particular angles and with an almost constant power.

In conditions that the system gain or the incident ray is not in the appropriate range, the system feedback comparator block apply the rotation command to the rotating plate and keeps the direction of the incident ray in the closest angle to the previous conditions fixed, [1], [2].

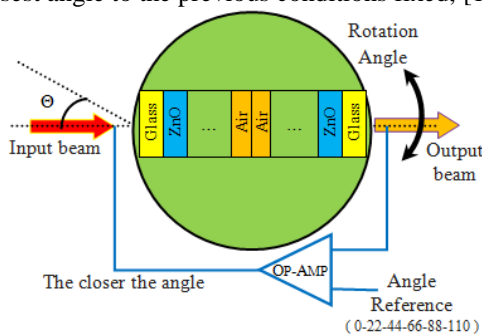


Fig.1. Structure block diagram with feedback.

II. FILM DEPOSITION AND INTRODUCING ZnO CRYSTAL STRUCTURES

The The sol-gel process is the transition of a liquid "sol" phase into a solid "gel" phase which with changing some parameters like temperature, speed, heat intensity, and pressure, sol can be produced. So, the preparation of an appropriate, smooth, and uniform sol will cause a uniform and pore-free film to be made.

Viscosity and density of the solution are considered the significant and effective parameters in producing a thin film which the prepared solution should have the molar ratio of Zn/ MEA. Thus, utilizing the sol-gel process, the solution consisting of 86% ml of Mono Ethanol Amine, 1/3 g of Zn (CH3COO) 2.2H2O, 15 ml of Isopropanol in 0.1 ml of water has been prepared. Considering the particular physical properties of this n-type semiconductor with the boiling point of 2360°C, the melting point of 1975°C, direct band gap of 3.38 eV, it has a gain and its hexagonal structure is the most stable one in these conditions. The compound is heated with a magnetic stirrer for 50 minutes in order for the transparent, uniform, and almost thick solution to be made. The solution is kept at the room temperature for 24 hours to make sure that there is no sediment[4].

The image of this film deposition is shown in figure 2 which using ultrasonic under the following conditions is made. The substrate in acid water for 20 minutes, in deionized water for 30 minutes, and in isopropanol for 20 minutes will be unpolluted and in a closed container will be completely dried.



Fig.2. Image of films after annealing.

About 0.2 to 0.5 of the solution for each film for 30 seconds will be spun at the speed of 3000 rpm (spin coating). The uniform and highly thin film formed at 275

°C for 10 minutes will be dried. The evaporation of water and isopropanol is at 50 °C to 100 °C and MEA is decomposed at 175 °C to 300 °C. these stages has to be repeated 10 times and finally the annealing will be done at 360 °C [3].

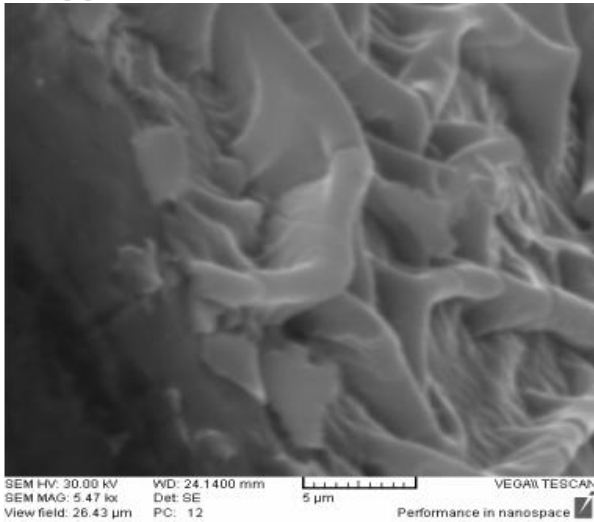


Fig.3. The image of secondary electron from the width of films.

In this project, the estimation of thickness using the non-optical profilometry (Alpha Step) the thickness of the ZnO thin film has been measured, which is shown in figure 4[3],[5].

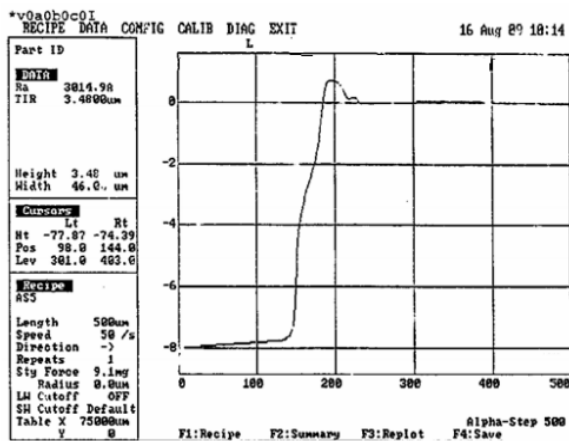


Fig.4. The result of the measurement of the thickness (Alpha Step).

Considering the above conditions, it is perceived that the thickness of each film is about 3500 Å (Angstrom) which depicts the production of a pleasant and favorable thin film using the spin coating method.

In the next stage, using X-ray diffraction (XRD), a crystal structure is obtained which is representing the c axis and the crystal plane (002) depicting that the designed layer is a polycrystalline structure. So, the pictures taken from the surface using Scanning Electron Microscopic (SEM), Atomic Force Microscopic (AFM), and Nanosurf method are shown in the sample figures 5 and 6.

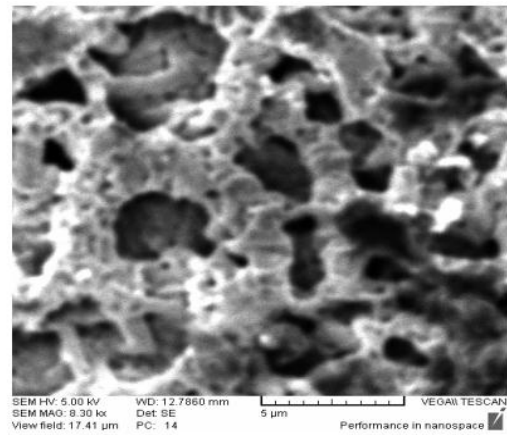
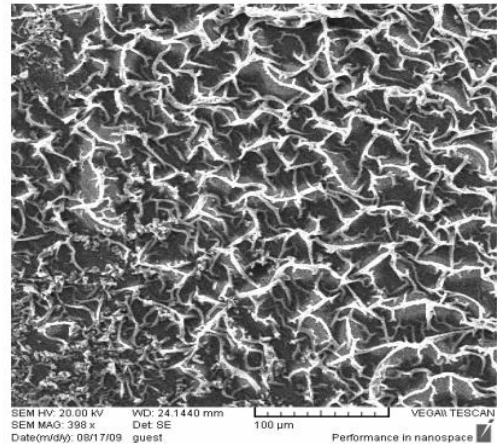


Fig.5. Secondary electron detector.

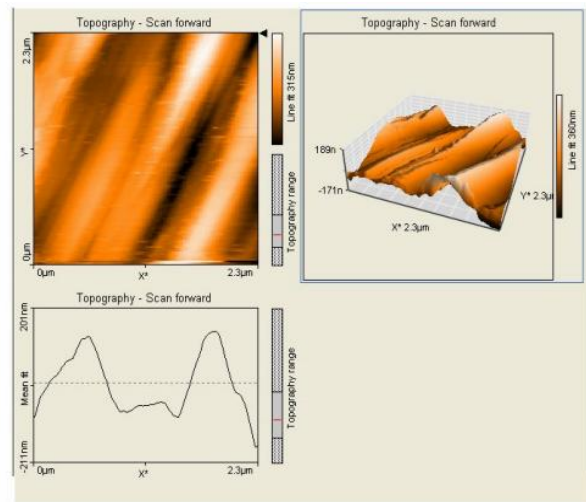


Fig.6. Atomic Force Microscope.

In the presented structure in this article, the 21 pairs of ZnO crystal layers, without applying apodization, have been exploited and utilized in a way that the failure coefficients, respectively from left to right, in the first 10 pairs of layers (from 1 to 10) have been considered $n_{Glass} = 1.45$, $n_{ZnO} = 2.0041$; in the two middle layers (11), the air gap, the failure coefficient is considered 1 ($n_{air} = 1$) and again continuously from left to right the failure coefficients are $n_{ZnO} = 2.0041$ and $n_{Glass} = 1.45$ [1], [2].



Fig.7. 21-layer periodic structure with defect

With regard to the above circumstances, to achieve the results of this kind of optical receivers in one-dimensional photonic crystal structures, TMM has been used [5]. Because the process has been analyzed in TE mode, with calculating dynamic matrix, the inverse of dynamic matrix, and dispersion matrix, the values of transmission bandwidth of optical receivers are investigated in the boundary conditions and TE mode [6],[11].

$$TE = \begin{cases} \frac{\partial Hz}{\partial y} = \frac{\partial Ex}{\partial t} + \partial Ex \\ -\frac{\partial Hz}{\partial x} = \epsilon \frac{\partial Ey}{\partial t} + \partial Ey \\ \frac{\partial Ey}{\partial x} - \frac{\partial Ex}{\partial y} = -\mu \frac{\partial Hz}{\partial x} - \sigma_m Hz \end{cases} \quad (1)$$

$$\begin{cases} M_{11} = \frac{1}{2} \left(1 + \frac{n_2 \cos \theta_2}{n_1 \cos \theta_1} \right) \cos \varphi + \frac{1}{2} i \sin \varphi \left(\frac{n_2 \cos \theta_2}{n_1 \cos \theta_1} + \frac{n_1 \cos \theta_1}{n_2 \cos \theta_2} \right) \\ M_{12} = \frac{1}{2} \left(1 - \frac{n_2 \cos \theta_2}{n_1 \cos \theta_1} \right) \cos \varphi + \frac{1}{2} i \sin \varphi \left(\frac{n_2 \cos \theta_2}{n_1 \cos \theta_1} - \frac{n_1 \cos \theta_1}{n_2 \cos \theta_2} \right) \\ M_{21} = \frac{1}{2} \left(1 - \frac{n_2 \cos \theta_2}{n_1 \cos \theta_1} \right) \cos \varphi - \frac{1}{2} i \sin \varphi \left(\frac{n_2 \cos \theta_2}{n_1 \cos \theta_1} - \frac{n_1 \cos \theta_1}{n_2 \cos \theta_2} \right) \\ M_{22} = \frac{1}{2} \left(1 + \frac{n_2 \cos \theta_2}{n_1 \cos \theta_1} \right) \cos \varphi - \frac{1}{2} i \sin \varphi \left(\frac{n_2 \cos \theta_2}{n_1 \cos \theta_1} + \frac{n_1 \cos \theta_1}{n_2 \cos \theta_2} \right) \end{cases} \quad (2)$$

$$M = \begin{bmatrix} M_{11} & M_{12} \\ M_{21} & M_{22} \end{bmatrix} = D_0^{-1} \left[\prod_{l=1}^N D_l P_l D_l^{-1} \right] D_s \quad (3)$$

$$D_l = \begin{bmatrix} 1 & 1 \\ n_l \cos \theta_l & -n_l \cos \theta_l \end{bmatrix}, P_l = \begin{bmatrix} e^{-i\phi_l} & 1 \\ 1 & e^{-i\phi_l} \end{bmatrix} \quad (4)$$

$$\phi_l = k_{lx} d_l \quad (4)$$

$$k_{lx} = n_l \frac{\omega}{c} \cos \theta_l \quad l = 0, 1, 2, \dots, N, S \quad (5)$$

$$T = \frac{n_S \cos \theta_S}{n_0 \cos \theta_0} |t|^2 = \frac{n_S \cos \theta_S}{n_0 \cos \theta_0} \left| \frac{1}{M_{11}} \right|^2 \quad (6)$$

Because detecting procedure in this design is intelligently based on the calculation of the input power, in particular angles of input signal; through measuring and comparing the values of the transmission band G(S) and the ray power P(S) in that range, the system feedback block prepares these conditions in such a way that with varying the factor K, the output gain of the detector will always remain the same; therefore, the system should always detect the incident ray in a bandwidth range of a constant wavelength and a constant power, that is, every signal incident upon the system will not have a favorable output and only the incident rays at particular angles will

be able to transit, which considering the frequency range of 4.65×10^{14} to 4.8×10^{14} , the angles are chosen [7],[10].

III. THE STRUCTURE OF AGC AND SIMULATION

So, with regard to the above explanations, the system transfer function and the circuit operation is like what is shown below:

$$\frac{Y(s)}{X(s)} = \frac{KP(s)G(s)}{1 + KP(s)G(s)H(s)} \quad (7)$$

A ray at a special angle is incident upon the filter and the filter output enters a comparator; if this output is the same as the defined output of the comparator, it will be permitted to exit; otherwise, there will be a feedback that enables the system to correct the ratio of the signal angle incident upon the filter in order for the output to be in the defined range.

The bandwidth and the transmission gain are the defined parameters of the comparator [8]. Thus, if the filter output does not include the needed gain and the favorable frequency range, it is not possible to exit.

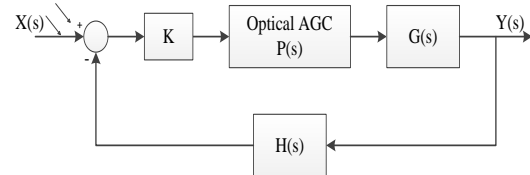


Fig.8. The block diagram of the circuit of the optical sensor.

Because this article is aimed at designing an optical sensor including the approximate bandwidth of 5 nm in the wavelength range of 630 nm to 635 nm, those angles are chosen which their output is in the mentioned range and the approximate area of the wave shape at the gain of -3dB is at least about 1 nm, for this reason, the approximate gain of the system in the range of this wavelength is more than 70% and the approximate area of 7.5×10^{-10} is acceptable for the comparator. As a result of this, the position of the structure in relation to the incident ray at the angles of 0° , 22° , 44° , 66° , 88° , 110° is favorable and is also calculated, which can be seen in the following figures [7],[12].

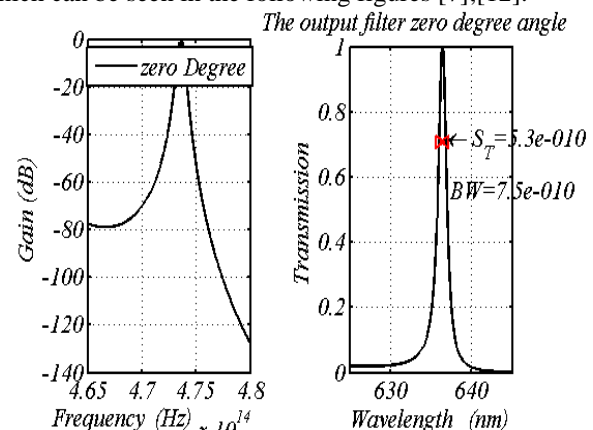


Fig.9. The receiver output at the angle of 0° .

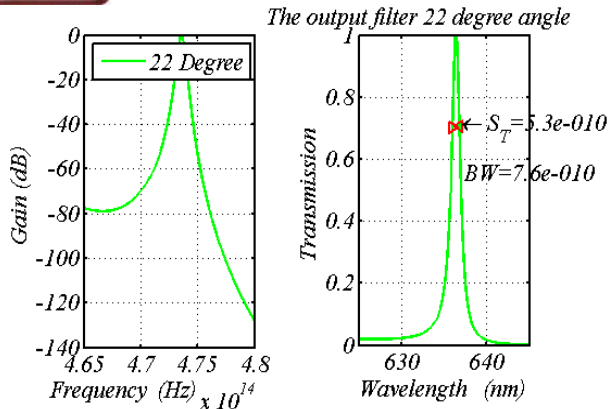


Fig.10. The receiver output at the angle of 22°.

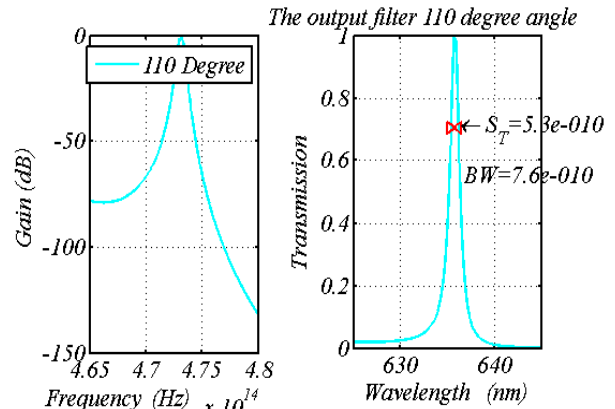


Fig.14. The receiver output at the angle of 110°.

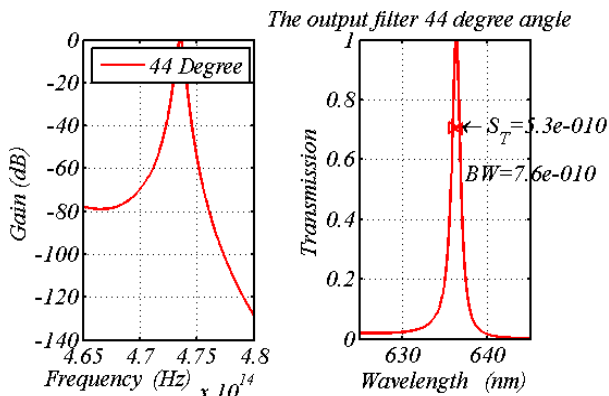


Fig.11. The receiver output at the angle of 44°.

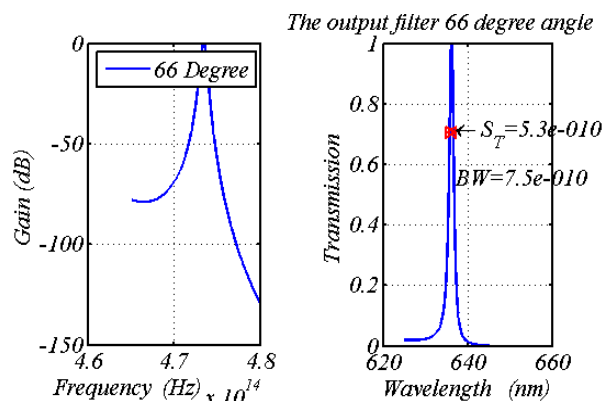


Fig.12. The receiver output at the angle of 66°.

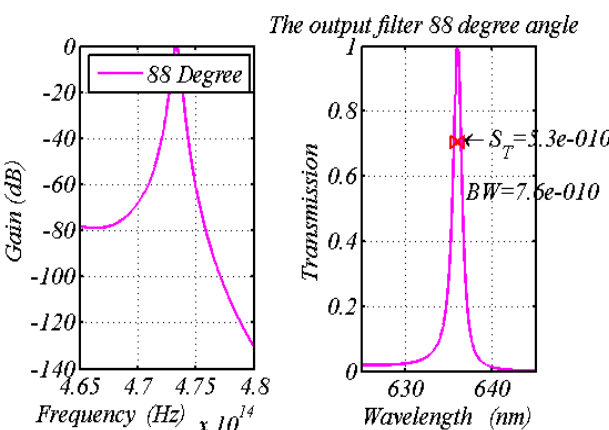


Fig.13. The receiver output at the angle of 88°.

Regarding the above mentioned explanations, if the signal is incident upon the structure at those mentioned angles, the output will have all the qualifications (only at the above angles the output will be qualified) and in this case, the system ranges of the frequencies, with the bandwidth of 300 GHz, will be 473 THz and 473.3 THz which can be seen in the figure 15.

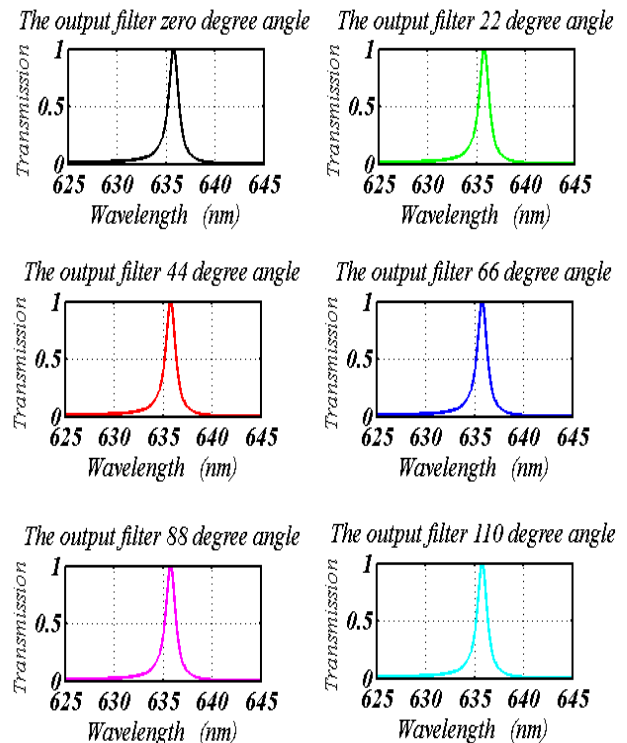


Fig.15. The outputs at the angles of 0°, 22°, 44°, 66°, 88°, 110°

CONCLUSION

In this project, a sensor and an optical AGC using one-dimensional photonic crystals have been designed that compared to other similar analog equipments have the advantages of the system high gain and a high-speed operation; according to this, if, for any reason, the signal angle incident upon the sensor varies, for instance, from 44° to 52°, the output will not be satisfactory and the comparator distinguishes it. Therefore, feedback structure

will change the signal angle into one of the favorable angles. As a result, the output having the acceptable power will not be out of the needed range and there will always exist the area of 5.3×10^{-10} and the bandwidth of 1 nm.

REFERENCES

- [1] G. Vijaya Prakash, K. Pradeesh, Ashwani Kumar, Rajesh Kumar, S. Venugopal Rao, M.L. Markham, J.J. Baumberg, "Fabrication and optoelectronic characterization of ZnO photonic structures", Elsevier, Materials Letters 62 (2008) 1183-1186.
- [2] A. Yamilov, X. Wu, and H. Cao, Photonic band structure of ZnO photonic crystal slab laser J. Appl. Phys. 98 103102 (2005).
- [3] Y.S. Park, C. W. Litton, T. C. Collins, and D.C. Reynolds, Exciton spectrum of ZnO Phys. Rev. 143 143(1966).
- [4] L. Znaidi, T. Touam, D. Vrel, N. Souded, S. Ben Yahia, O. Brinza, A. Fischer and A. Boudrioua, "ZnO Thin Films Synthesized by Sol-Gel Process for Photonic Applications", Proceedings of the International Congress on Advances in Applied Physics and Materials Science, Antalya 2011.
- [5] A. Rostami and S. Matloub, "Optical Filter Characteristics Control Using Chirped Homogeneous Fibonacci-Class Multilayer Stacks", Laser Physics, Vol. 14, No. 12, 2004, pp. 1475-1482.
- [6] S. Olyaei, M. Soroosh, and M. Izadpanah, "Transfer matrix modeling of avalanche photodiode", Frontiers of Optoelectronic, Vol. 5, No. 3, pp. 317-321, 2012.
- [7] R. Khodadadi, M. A. Ghasemi, H. A. Banaei, "Adjustable Filters For Optical Communications Systems Based On One Dimensional Photonic Crystal Structures," International Journal of Engineering Research and Applications (IJERA), 2012, Vol. 2, pp. 272-276.
- [8] S. Mohammad Nejad and S. Olyaei, "Low- Noise High-Accuracy TOF Laser Range Finder", American Journal of Applied Sciences 5 (7): 755-762, 2008.
- [9] Reza Khodadadi, Mir Ali Ghasemi, Hamed Alipour Banaei, "Adjustable Filters For Optical Communications Systems Based On One Dimensional Photonic Crystal Structures," International Journal of Engineering Research and Applications (IJERA), 2012, Vol. 2, pp. 272-276.
- [10] A. Rostami, H. Alipour Banaei, F. Nazari, A. Bahrami, An ultra compact photonic crystal wavelength division demultiplexer using resonance cavities in a modified Y-branch structure, Optik 122 (2011) 1481-1485.
- [11] J.D. Joannopoulos, R.D. Meade, J.N. Winn, Photonic Crystals: Molding the Flow of Light, (Princeton University Press, Princeton, 1995), (2nd edition, 2008).
- [12] J.B. Chen, Y.S. W. Xi Zhou, Y.X. Zheng, H.B. Zhao and L.Y. Chen, Comparison Study of the Band-gap Structure of a 1D-Photonic Crystal by Using TMM and FDTD Analyses, Journal of the Korean Physical Society, Vol. 58, No. 4, April 2011, pp. 1014-1020.

AUTHOR'S PROFILE



Reza Khodadadi

was born in Tehran, Iran, in 1975. He received the B.Sc. and M.Sc. degrees in electrical engineering, electronics, Islamic Azad University, Karaj branch, Karaj, Iran and Islamic Azad University, Ahar, Iran, in 2000 and 2012, respectively. His research interests include Strengthening the Optical Sensors, Photonic Crystals, Laser, Wireless Networks, LNA, Audio Mixers, RF Application, Signal Processing and Artificial Intelligence. Mr. Khodadadi is a lecturer in Islamic Azad University, Karaj Branch, Karaj, Iran.
Email: ur_khodadadi@yahoo.com

Samaneh Khodadadi

Was born in Tehran, in 1986. He received the B.Sc. degree in Physics, University of Science and Technology, Tehran, Iran in 2010, research interests. His combination of chemical, photonic crystals, lasers, photonics, optical signal processing and artificial intelligence.